ChemPubSoc Europe
DOI: 10.1002/chem.201501721
CHEMISTRY
A European Journal
Full Paper

Energetic Materials |*Hot Paper*|

Crystal Engineering of Energetic Materials: Co-crystals of Ethylenedinitramine (EDNA) with Modified Performance and Improved Chemical Stability

Christer B. Aakeröy,* Tharanga K. Wijethunga, and John Desper[a]

Abstract: In the area of energetic materials, co-crystallization is emerging as a new technology for modifying or enhancing the properties of existing energetic substances. Ethylenedinitramine (EDNA) is a known energetic material which requires attention partly due to its chemical instability originating with its two highly acidic protons. In order to stabilize EDNA, a co-crystallization approach targeting the acidic protons using a series of co-crystallizing agents with suitable hydrogen-bond acceptors was employed. Fifteen attempted co-crystallizations resulted in eight successful outcomes and six of these were crystallographically characterized and all showed evidence of hydrogen bonds to the intended protons. Calculated detonation properties and experimental thermal and impact data for the co-crystals were obtained and compared with those of pure EDNA. The co-crystal of EDNA and 1,2-bis(4-pyridyl)ethylene was recognized as a more thermally stable alternative to EDNA while the co-crystal of EDNA and pyrazine *N*,*N*′-dioxide showed comparable detonation strengths (and much improved chemical stability) compared with that of EDNA. The co-crystals EDNA:4,4′-bipyridine and EDNA:pyrazine *N*,*N*′-dioxide were found to be about 50 % less impact sensitive than EDNA, all of which illustrate how co-crystallizations can be utilized for successfully modifying specific aspects of energetic materials.

Introduction

Energetic materials contain substantial amounts of stored energy that can be released rapidly,[1] and representatives of energetic materials include explosives, propellants and pyrotechnics.[2] Even though a large number of different energetic compounds are known in armaments, mining, fireworks and space explorations,[3] many have drawbacks leading to restrictions or limitations of their use.[4] Common problems include excessive sensitivity to impact, heat, shock or friction[5] (e.g., RDX[6] and CL-20[7]), as well as undesirable reactivity towards different environmental factors (e.g., nitramine explosives[8]), and high toxicity.[9] Highly powerful energetic materials inherently display high sensitivity and/or high reactivity leading to a power-safety contradiction[10] and, consequently, designing powerful energetic materials with improved safety and stability is a major challenge.[11]

The pursuit of new energetic materials typically follows one of two approaches. First, a completely new molecule or salt can be prepared[12] in order to uncover a material with the required properties such as high power, low sensitivity and low reactivity expressed in an integrated manner,[13] but optimizing all these properties within a finite time scale is enormously difficult.[14] An alternative avenue may be found through the use of co-crystal technology[15] wherein a known energetic material is combined with either an energetic or a non-energetic compound[16] via noncovalent interactions within a crystalline framework.[17] Co-crystallizations can provide means for altering a range of properties that are a function of the nature of the solid state, such as density, mechanical and thermal stability, and solubility which can all facilitate the pursuit of safer or more versatile energetic materials.[18] More generally, co-crystallizations may also offer an avenue for stabilizing liquids and other volatile chemicals[19] thereby lowering the risk of exposure through inhalation of toxic energetic materials[20] (many nitro-containing compounds are toxic). All in all, a co-crystal version of an energetic material can, in certain circumstances, be more useful because of superior chemical stability and shelf-life even though it may have slightly lower energetic performance.

Ethylenedinitramine (EDNA) also known as Haleite[21] (Figure 1), is described as the first entirely American high explosive.[22] EDNA combines the properties of a high explosive like TNT and an initiating agent like mercury fulminate, possessing a high brisance, comparatively low impact sensitivity and high heat sensitivity. This compound is applied as a secondary explosive, booster explosive and in the preparation of cast explosives such as ednatol.[23]

An important reason behind some difficulties in the use of EDNA is its relatively high chemical reactivity, a common drawback associated with many nitramine-based explosives.[24] Overly acidic compounds are often prone to chemical instabili-

---

[a] Prof. C. B. Aakeröy, T. K. Wijethunga, Dr. J. Desper
Department of Chemistry, Kansas State University
Manhattan, KS, 66506 (USA)
E-mail: aakeroy@ksu.edu

Supporting information for this article is available on the WWW under http://dx.doi.org/10.1002/chem.201501721.

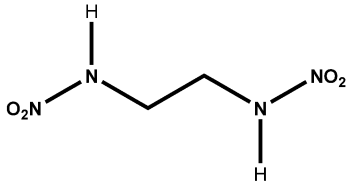

Figure 1. Chemical structure of EDNA.

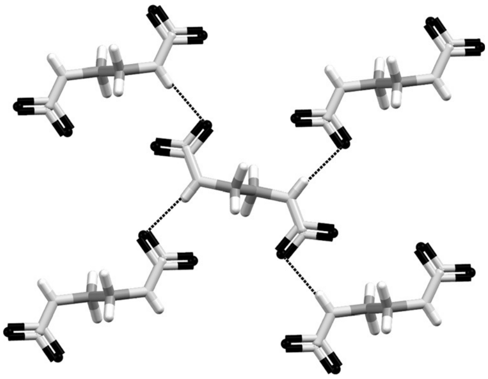

Figure 2. Part of the crystal structure of EDNA with hydrogen bonds between nitro oxygen atoms and acidic amine protons.[33]

ty and hygroscopicity,[25] which can create problems with transport, processing, and storage. For example, tetranitropyrole is unstable at ambient temperatures[26] and dinitrotriazole is deliquescent,[27] and both contain an acidic N–H moiety. The highly acidic picric acid, another well-known explosive, is corrosive and reacts readily with metals to form shock-sensitive salts. EDNA is also highly acidic[28] (pK_{a1} 5.31 and pK_{a2} 6.64),[29] due to the ease of delocalization, facilitated by the nitro groups, of the remaining negative charge upon deprotonation; thus EDNA is corrosive and can react with metals and metal salts[30] to produce new materials with unpredictable properties. For example, Cu^{II}EDNA, is easily synthesized and has low impact sensitivity[31] whereas Pb^{II}EDNA displays superior properties/performance compared to EDNA itself.[32]

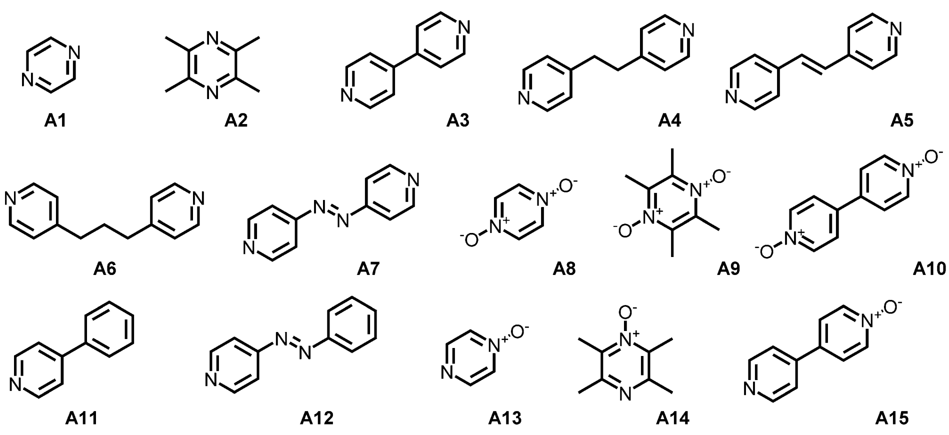

Scheme 1. Hydrogen-bond acceptors used in this study.

In this study, we describe the use of co-crystallizations for altering the physical properties and stability of EDNA while retaining some valuable characteristics associated with an energetic material. The goals of this study are to establish: 1) if EDNA is a suitable target for co-crystal synthesis; 2) if the acidic protons can be engaged (and essentially protected) by hydrogen bonding to suitable co-formers; 3) if any explosive property of the resulting materials can be modulated in a useful manner; and 4) if the chemical stability of EDNA can be improved through co-crystallizations.

A close look at the crystal structure of EDNA[33] (Figure 2) reveals that these acidic protons are interacting with nitro oxygen atoms which are considered to be poor hydrogen-bond acceptors.

With this in mind we selected fifteen hydrogen-bond acceptors that potentially would compete successfully with the nitro groups for the attention of the acidic protons (Scheme 1), including N-based acceptors (**A1**–**A7**, **A11** and **A12**) O-based acceptors (**A8**–**A10**) and mixed N- and O-based acceptors (**A13**–**A15**). These 15 acceptors can be further categorized as symmetric ditopic (**A1**–**A10**), monotopic (**A11** and **A12**) and dissymmetric ditopic (**A13** to **A15**). The reason for selecting primarily ditopic acceptors (all but **A11** and **A12**) was first of all that we wanted to aim for some degree of structural consistency; a combination of a ditopic donor and a ditopic acceptor is likely to produce infinite supramolecular chains. Second, the N-oxides are likely to form the same hydrogen-bonded motifs as the parent N-heterocycles but with a better oxygen balance which would be beneficial from a performance perspective.

Results

Initial co-crystal screening was carried out by combining EDNA and the acceptors (Scheme 1) in stoichiometric ratios and the products obtained were analyzed with both IR spectroscopy and DSC. The solvent of choice was methanol as both EDNA and the acceptors showed comparable solubility in alcohols. Eight of fifteen attempts yielded co-crystals as indicated by both IR and DSC (see the Supporting Information) data. Although vibrational spectroscopy provides information about whether a co-crystal has formed or not, it does not reveal to what extent the amine protons on EDNA participate in hydrogen bonding. To address this issue, crystallographic data are needed and six of the eight new co-crystals were characterized using single-crystal X-ray diffraction.

Crystallographic data for the six co-crystals (**EDNA:A3**, **EDNA:A4**, **EDNA:A5**, **EDNA:A7**, **EDNA:A8** and **EDNA:A12**) are

Table 1. Hydrogen bond geometries for six crystal structures.

Co-crystal	D–H···A	D–H [Å]	H···A [Å]	D···A [Å]	D–H···A [°]
EDNA:A3	N(12)-H(12)···N(21)	0.95(18)	1.85(19)	2.787(19)	169.6(15)
	N(15)-H(15)···N(31)#1	1.5(18)	1.74(18)	2.788(19)	176.9(15)
EDNA:A4	N121-H121···N211	0.83(2)	1.98(2)	2.780(2)	164(2)
	N122-H122···N212	0.97(2)	1.82(2)	2.770(2)	169.2(17)
EDNA:A5	N(12)-H(12)···N(21)	0.89(2)	1.87(2)	2.747(2)	167.5(19)
EDNA:A7	N(12)-H(12)···N(21)	0.92(15)	1.93(15)	2.841(12)	175.0(13)
EDNA:A8	N(12)-H(12)···O(21)	0.90(18)	1.86(18)	2.720(13)	159.4(16)
EDNA:A12	N(12)-H(12)···N(21)	0.92(17)	1.89(17)	2.818(17)	176.4(16)

EDNA:A3 #1: $-x+1, y-1, -z+1/2$; **EDNA:A4** #1: $-x+1, -y+1, -z+2$; #2: $-x+2, -y+2, -z+1$; #3: $-x+2, -y+1, -z+1$; #4: $-x+1, -y, -z+2$; **EDNA:A5** #1: $-x+1, -y+1, -z+1$; #2: $-x, -y, -z$; **EDNA:A7** #1: $-x, -y+1, -z$; #2: $-x+2, -y+1, -z+1$; **EDNA:A8** #1: $-x, -y, -z+1$; #2: $-x+1, -y+1, -z$; **EDNA:A12** #1: $-x+1/2, -y+3/2, -z+1$.

reported in the Supporting Information and hydrogen bond geometries are summarized in Table 1.

The crystal structure of **EDNA:A3** (Figure 3) reveals a 1:1 stoichiometry where the two components are connected via primary N–H···N(py) hydrogen bonds. As intended, the pyridine-based acceptor sites have provided a successful replacement for the N–H···O(nitro) hydrogen bonds present in the crystal structure of EDNA itself.

Somewhat surprisingly though, the molecular geometry of EDNA molecules in the **EDNA:A3** lattice is very different when compared to their molecular conformations in the crystal structure of EDNA by itself (Figure 2).

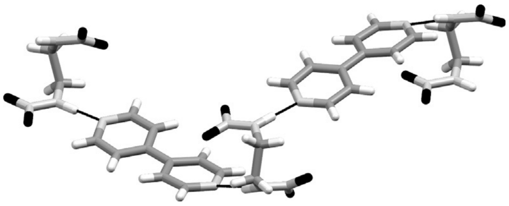

Figure 3. Primary interactions in the **EDNA:A3** co-crystal.

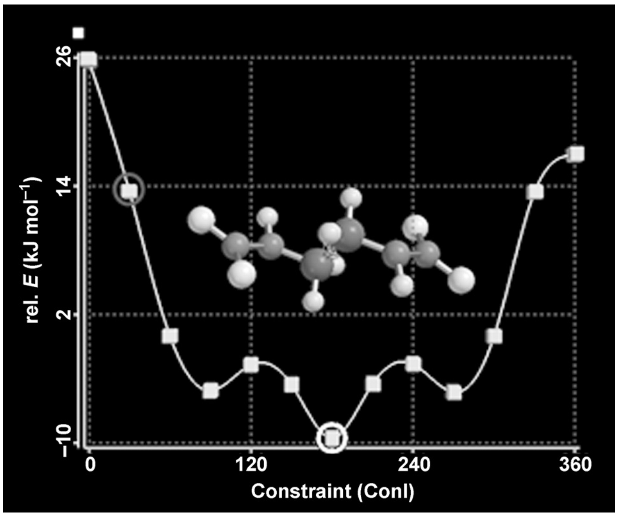

Figure 4. Relative energies of EDNA as a function of the N-C-C-N torsion angle (changed from 0° to 360° with 30° increments). The observed torsion angle in the solid of pure EDNA is 180° whereas it is 28° in the co-crystal **EDNA:A3**.

The N-C-C-N torsion angle for EDNA in **EDNA:A3** is 28°, while it is 180° for pure EDNA. In order to find the energy difference between the two orientations, a molecular structure optimization was subsequently performed. A plot of energy versus torsion angle (Figure 4) shows that the energy difference between the two conformations is about 24 kJ mol^{-1}, favoring the molecular structure observed in the EDNA crystal structure. It is reasonable to assume that the relatively small energy differences can readily be compensated for by the new N–H···N(py) hydrogen bonds that are observed in the structure of **EDNA:A3**.

The crystal structure of **EDNA:A4** (Figure 5) reveals the expected N–H···N(py) hydrogen bonds and the two components are again present in a 1:1 ratio. In this structure the EDNA molecules adopt a 180° torsion angle of the N-C-C-N backbone (the molecule is located on a crystallographic special position).

The crystal structure of **EDNA:A5** (Figure 6) shares the main structural features with those found in the structure of **EDNA:A4** with a 1:1 stoichiometry, structure directing N–H···N(py) hydrogen bonds resulting in infinite chains, and a 180° torsion angle of the N-C-C-N backbone of EDNA.

Although 4,4′-azopyridine, the co-former in **EDNA:A7**, does contain two additional nitrogen atoms that, in theory, could engage with the acidic protons of EDNA, the two π-sites are substantially better acceptors[34] (Figure 7) and consequently, N–H···N(py) driven hydrogen-bonded chains dominate the crystal structure, similar to what was found in both **EDNA:A4** and **EDNA:A5**. The stoichiometry again is 1:1 which is dictated by the fact that EDNA has two strong donors which are matched by the two main N(py)-acceptor sites on **A7**.

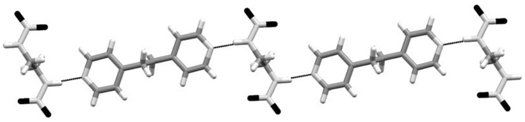

Figure 5. Primary hydrogen bonds in the **EDNA:A4** co-crystal.

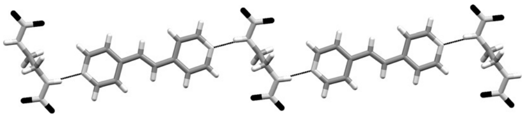

Figure 6. Part of the infinite hydrogen-bonded chain in the **EDNA:A5** co-crystal.

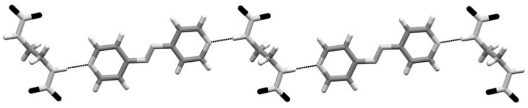

Figure 7. Primary hydrogen bonds in the **EDNA:A7** co-crystal.

The crystal structure of **EDNA:A8** (Figure 8) shows a 1:1 stoichiometry, and infinite hydrogen bonds generated by N–H···O-N(py) chain formation between the oxygen atoms of N-oxide and the acidic N–H protons of EDNA. This structure illustrates that EDNA is capable of forming co-crystals not only with N-based acceptors but also with O-based acceptors via the acidic protons.

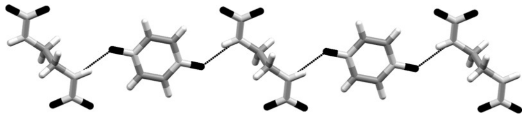

Figure 8. Primary interactions in the **EDNA:A8** co-crystal.

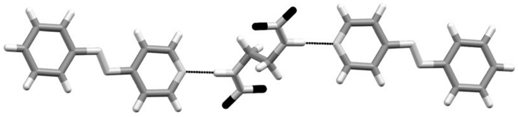

Figure 9. Main hydrogen bonds in the **EDNA:A12** co-crystal.

The final crystal structure obtained in this series was with a monotopic hydrogen-bond acceptor, **A12**, and consequently the stoichiometry in this case is 1:2 (**EDNA:A12**; Figure 9). The chains that resulted when ditopic acceptors were combined with EDNA is now replaced with a discrete trimeric motif.

Thermal analysis

The thermal analysis of the eight co-crystals was mainly focused on three aspects; melting temperature, decomposition temperature, and enthalpy of decomposition, and the results were compared with that of EDNA. As an example, Figure 10 shows the DSC trace for **EDNA:A7**.

The results are summarized in Table 2 (see the Supporting Information for DSC curves). Pure EDNA has a melting point of 180 °C and decomposes at 186 °C accompanied by a 1971(±18) J g^{-1} release of energy (for comparison the corresponding energy release for HMX is 1987 J g^{-1}[35]).

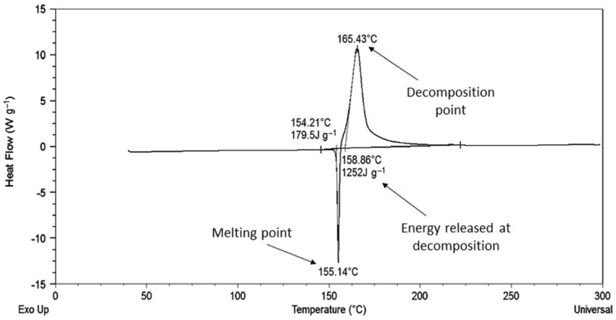

Figure 10. DSC trace for **EDNA:A7** co-crystal.

Performance analysis

The detonation properties of the six co-crystals were calculated using experimental densities obtained from the single-crystal structure determinations. Detonation velocities and pressures were calculated using nitrogen equivalents of different detonation products,[36] and oxygen balances were calculated using well-established methods.[37] Table 3 summarizes the detonation properties for the six co-crystals. The oxygen balance of an explosive is the mass of oxygen either in excess or in deficit of that required for the complete oxidation of the carbon and

Table 2. Thermal properties of co-crystals.

Compound/ co-crystal	Co-former melting point [°C]	Co-crystal melting point [°C]	Melting enthalpy [J g^{-1}]	Decomposition point [°C]	Energy released at decomposition [J g^{-1}]
EDNA	–	180	215 ± 5	186	1971 ± 18
EDNA:A3	112–114	146	145 ± 11	189	1055 ± 11
EDNA:A4	110–112	129	133 ± 14	191	985 ± 3
EDNA:A5	148–152	–	–	198	955 ± 23
EDNA:A6	53–56	118	119 ± 5	194	769 ± 31
EDNA:A7	106–110	154	160 ± 28	165	1242 ± 15
EDNA:A8	285–289	156	150 ± 7	172	1447 ± 14
EDNA:A11	69–73	94	198 ± 2	203	1214 ± 37
EDNA:A12	96–99	133	121 ± 4	168	982 ± 18

Melting enthalpies and decomposition enthalpies are reported as an average from two trials for each compound with the calculated standard deviation.

Table 3. Detonation properties of co-crystals.

Compound/ co-crystal	Density [g cm^{-3}]	Detonation velocity[a] [km s^{-1}]	Detonation pressure[a] [GPa]	Oxygen balance[a]
EDNA	1.65 (RT)	7.890	26.72	−32
EDNA:A3	1.489 (120 K) 1.452 (RT)	6.178	15.24	−141
EDNA:A4	1.407 (120 K) 1.355 (RT)	5.967	13.70	−158
EDNA:A5	1.460 (120 K) 1.434 (RT)	6.030	14.32	−154
EDNA:A7	1.529 (120 K)	6.504	17.21	−129
EDNA:A8	1.68 (120 K) 1.64 (RT)	7.256	22.73	−67
EDNA:A12	1.432 (120 K)	5.948	13.75	−173

[a] All the velocity and pressure calculations for the co-crystals were carried out using low temperature densities while for EDNA the calculations were conducted using room temperature density.

hydrogen atoms present in the explosive.[38] A negative balance means that there is an insufficient amount of oxygen for complete combustion. EDNA has an oxygen balance of −32% and the co-crystals of EDNA presented here all have a more negative oxygen balance with **EDNA:A8** at −67% being the least unfavorable (for comparison TNT has an oxygen balance of −74%).

The impact sensitivities of EDNA, **EDNA:A3**, and **EDNA:A8** were examined using conventional drop-weight measurements and calculated using Bruceton analysis. The H_{50} values are 99(±1), 140(±1), and 138(±1) cm, respectively, where a higher value indicates reduced sensitivity.

Discussion

In all six crystal structures the targeted acidic N–H protons did form hydrogen bonds with the acceptors resulting in successful co-crystallization. In five of the six structures, **EDNA:A3** being the exception, the EDNA molecule adopted the most favorable molecular geometry with 180° torsion angle of the N-C-C-N backbone. Another supramolecular synthetic target in this study was to achieve some structural consistency through the use of ditopic hydrogen-bond acceptors. In four of the five crystal structures of EDNA with ditopic acceptors (**A3**, **A4**, **A5**, **A8**) the result was an infinite hydrogen-bonded chain of alternating EDNA:co-former components, and the zig–zag shaped chain found in the crystal structure of **EDNA:A3** was due to the unusual conformation of the backbone of the EDNA molecules in that particular solid.

Out of fifteen co-crystallization attempts eight formed co-crystals successfully. In order to explain the reason behind the successes and failures, we analyzed the electrostatic potentials of each acceptor atom. By looking at the electrostatic potential values of N-based acceptors it was evident that the higher value of electrostatic potential on the acceptor lead to co-crystal formation, where **A1** and **A2** being the molecules with least potential, did not show any evidence of successful interactions. But this explanation only seems to be valid with N-based acceptors only. When considering the O-based and mixed acceptors, it seems even the higher potential on the acceptor atoms are not successful in forming hydrogen bonds with EDNA.

The melting points for six of the eight co-crystals of EDNA fall between those of the two pure components of each co-crystal (Figure 11). **EDNA:A8** has a lower melting point than both initial compounds while **EDNA:A5** has a decomposition temperature approximately twenty degrees higher than the melting point of EDNA, and about ten degrees above its decomposition temperature. As mentioned previously, a drawback with EDNA is a relatively high sensitivity to heat, which means that the co-crystal **EDNA:A5** offers an improvement in this respect.

The relationship between molecular structure and melting point of the corresponding solid is governed by a delicate balance between numerous intermolecular interactions and it is largely unpredictable. However, a systematic co-crystallization approach, can provide some trends and correlations between molecular structure and properties even in heteromeric solids as long as the primary structural features are somewhat consistent from one compound to the next.

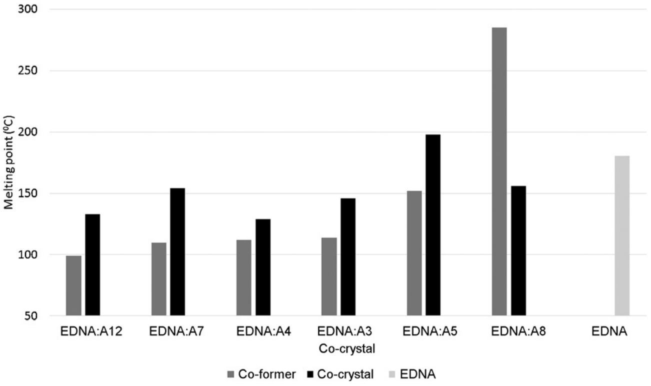

Figure 11. Co-crystal and co-former melting points.

Despite the lack of strong correlation between the two variables (which should not be expected), the general trend indicates that the co-former exercises an influence on the solid form of EDNA that can be estimated reasonably well.

Density is a major contributor to the explosive properties of an energetic material.[39] Therefore, we examined whether there was any correlation between the density of the pure co-former and the density of the corresponding EDNA co-crystal thereof (Figure 12 and Figure 13). The analysis was carried out only for the co-crystals where the room temperature densities are reported for the co-formers.

EDNA:A8 has a comparable density (1.64 g cm^{-3} vs. EDNA 1.65 g cm^{-3}). As was the case with the melting points of the EDNA co-crystals, there is, generally speaking, an increase of density of the co-crystal as the density of the co-former goes up (**EDNA:A5** is a slight anomaly) and the big improvement is seen in the co-crystal with an N-oxide based co-former, **A8**.

The use of N-oxides as co-formers serves two purposes when it comes to designing and synthesizing energetic co-crystals. The oxygen balance is obviously benefitting by moving from a parent N-heterocycle to the corresponding N-oxide, but the density can also improve.[40] In order to examine how general this second point is, we compared densities of

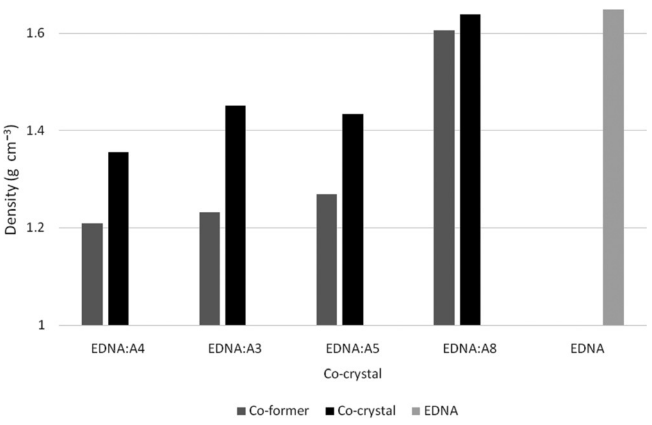

Figure 12. Co-crystal and co-former densities at room temperature.

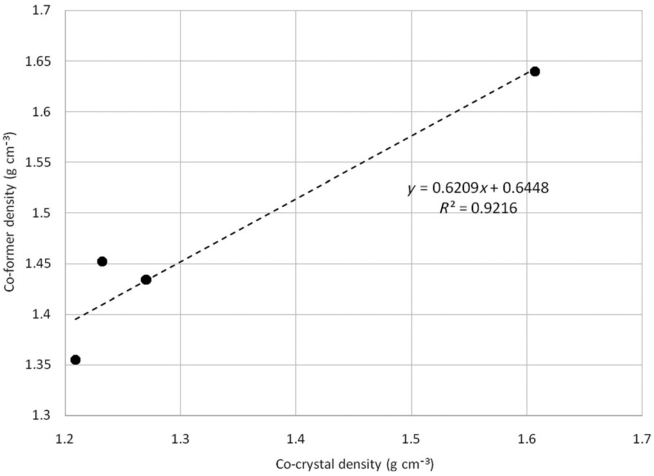

Figure 13. Correlation between co-crystal and co-former densities at room temperature.

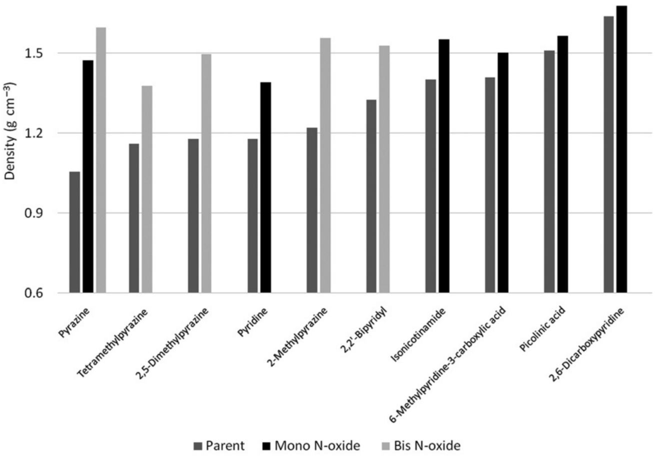

Figure 14. Densities of N-heterocyclic compounds and their corresponding mono- or bis-N-oxides.

ten N-heterocyclic compounds and their corresponding mono- and/or bis-N-oxides[41] (Figure 14).

Although this data set may not be very large, the general trend is nevertheless clear and unambiguous. In each case, the oxidized species displays a higher density (as determined by single-crystal X-ray diffraction) than the parent N-heterocycle and the increases range from a few percent to almost 50% in the case of pyrazine versus pyrazine bis-N-oxide. The types of compounds in this series also span a large range and include molecules decorated with a variety of functional groups. Against this background, it is not surprising then that the EDNA co-crystal with a density that is comparable to EDNA itself involves pyrazine bis-N-oxide as the co-former. Furthermore, it may be particularly worthwhile to examine N-oxides as co-formers in future strategies geared towards enhancing the density of heteromeric energetic materials.

In this systematic approach, structural consistency was a desired outcome as we could then also expect a positive correlation between packing coefficient and density (no heavy atoms beyond nitrogen and oxygen were present in any of the co-formers). To verify this hypothesis we plotted the two parameters against each other (Figure 15).

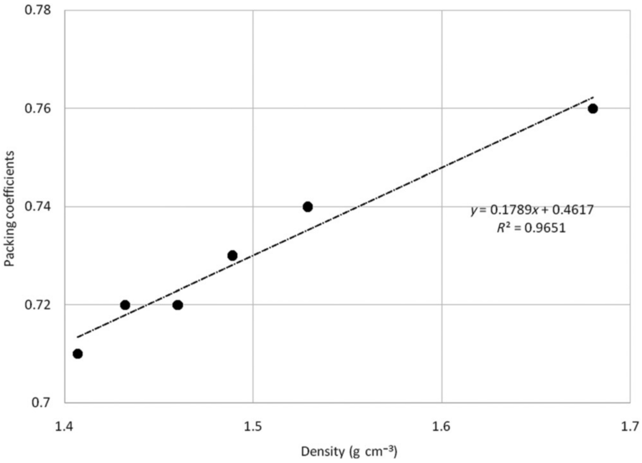

Figure 15. A plot of packing coefficient versus density in six EDNA co-crystals.

As shown, the packing coefficient provides an excellent indication of density of the resulting lattice.

Among the eight co-crystals **EDNA:A8** gives the highest enthalpy change upon decomposition (as determined by DSC) which is likely related to the influence of the co-former, **A8**, which has a more favorable oxygen balance than any of the co-formers used in this study.[42] The DSC analysis also shows that there is a relatively large temperature difference between the melting and decomposition temperature in **EDNA:A6** and **EDNA:A11** compared to the same parameter in pure EDNA. This means that the window of stability beyond the melting point can be substantially improved upon co-crystallization. It is particularly interesting to note that the molten phase of **EDNA:A11** shows a stability beyond that of the decomposition temperature of EDNA itself which indicates that some critical intermolecular interactions remain intact in the liquid phase.

EDNA is considered to be an energetic compound with relatively low sensitivity to impact and friction and this is a property that helps to determine if a material is suitable as a primary or secondary explosive as well as what kind of precautions are needed for storage and handling. Any incorporation of EDNA within a new crystalline material is likely to impact sensitivity, broadly speaking, as well as any property governed by the nature of the solid state. We examined the impact sensitivity of two co-crystals in this series with particularly favorable thermal stability (**EDNA:A3**) and energetic properties (**EDNA:A8**) and the two co-crystals were significantly less impact sensitive than EDNA itself. The co-formers in the lattice can essentially be viewed as acting as buffers or barriers between the inherently unstable energetic molecules which consequently improves the sensitivity.

The acidity of pure EDNA makes it corrosive and prone to react with metals which can restrict processability and shelf-life. Furthermore, the sensitivity of the products formed can create a completely new set of unpredictable and undesirable challenges. One reason for co-crystallizing EDNA with molecules capable of binding to the acidic protons was to introduce a "supramolecular protecting group" that might reduce the chemical reactivity of EDNA thereby making it more stable. In order to test the validity of this approach, we carried out a simple qualitative test where EDNA and **EDNA:A8**, respectively, were sprinkled in a slurried form (with a few drops of methanol) directly onto strips of copper metal (Figure 16).

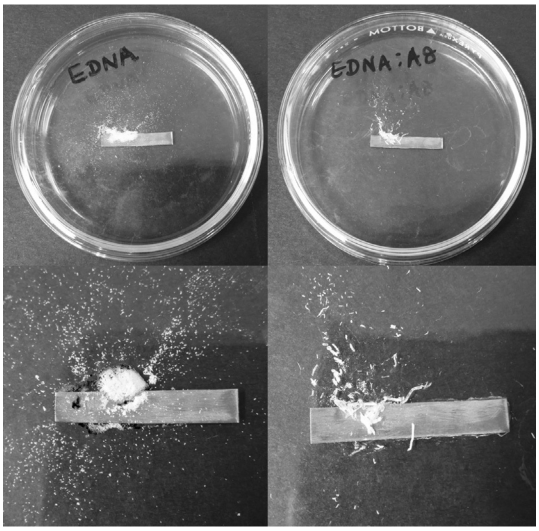

Figure 16. A slurry of EDNA (top left) and **EDNA:A8** (top right), in contact with copper metal. Notable corrosion of the metal was observed after 20 h in the case of pure EDNA (bottom left) but no visible change to the copper metal took place with **EDNA:A8** under the same conditions (bottom right).

The corrosive nature of EDNA is clearly manifested even after a relatively short amount of time (20 h) at ambient temperature, whereas the **EDNA:A8** solid form does not display any noticeable degrading of the copper metal. Much more work needs to be done in order to accurately quantify the damaging effect that the EDNA–metal system is experiencing and we also intend to look more broadly at the potential differences that EDNA and co-crystals thereof may have on materials that are likely to be used in processing, storage and formulation of energetic materials of this type.

Conclusions

A systematic co-crystallization study of EDNA has demonstrated that the acidic protons in the energetic material can be successfully targeted with suitable hydrogen-bond acceptors. Six of the eight co-crystals synthesized were characterized using single-crystal diffraction and the outcome was predictable supramolecular motifs based upon N–H···N and N–H···O structure-directing hydrogen bonds. The co-formers also act as "supramolecular protecting groups" resulting in a reduced chemical instability/corrosiveness which is otherwise detrimental to the storage and processability of EDNA. Thermal properties, impact sensitivity, and detonation velocities and pressure could also be modified and altered with a degree of predictability since the structural consistency throughout this series unearthed some correlations between molecular structure/property of the pure co-former and the physical properties performance of the resulting energetic co-crystal. This clearly suggests that systematic co-crystallizations may allow us to fine-tune properties that are important for storage, handling, and processing, with minimal negative impact on the eventual energetic behavior of the targeted substance.

Experimental Section

All the precursors, solvents and acceptors **A1**–**A6** and **A11** were purchased from commercial sources and were used without further purification. EDNA was synthesized following a reported procedure.[43] **A8**–**A10** and **A13**–**A15** were synthesized following previously reported procedures.[44] **A7**[45] and **A12**[46] were also synthesized following reported procedures. ^{1}H NMR spectra were recorded on a Varian Unity plus 400 MHz spectrometer. Infrared spectra were recorded with a Nicolet 380 FT-IR. Differential scanning calorimetry (DSC) measurements were carried out on a Q20, TA Instruments using Tzero aluminum pans under nitrogen (50.0 mL min^{-1}) purge at a heating rate of 5 °C min^{-1} over a range of 20–300 °C.

Standard protocols for handling energetic materials were followed at all times.[47] All synthesis and handling of EDNA was carried out inside a fume hood and nonmetallic spatulas were used when measuring EDNA. Kevlar gloves, laboratory coat and goggles were worn at all times. Mechanical actions involving scratching or scraping were avoided and EDNA was synthesized only in small amounts.

Synthesis of EDNA

A round-bottom flask was equipped with a stir bar and 7 mL of 90% nitric acid (fuming nitric acid) under nitrogen atmosphere and cooled to 0 °C. To this, 2.0 g of ethylene urea (2-imidazolidone) was added portion-wise while keeping the temperature below 20 °C. The reaction mixture was stirred under these conditions for 1 h and subsequently allowed to warm to room temperature. The reaction mixture was then quenched with iced water and the precipitate that formed was collected by filtration.

The precipitate was added to about 50 mL of boiling water in small portions and the temperature of water was maintained until no more gas evolution was seen. Then the aqueous solution was cooled in an ice bath and the precipitated desired product was collected by filtration as a white crystalline powder in 55% yield. Melting point 178–180 °C (reported 174–178 °C);[48] ^{1}H NMR (δ_H; DMSO, 400 MHz): 12.12 (s br, 2 H), 3.59 ppm (s, 4 H).

Theoretical calculations

Geometry optimizations of EDNA at various fixed torsion angles were carried out with DFT calculations at the B3LYP/6-31G* level of theory using Spartan'08.[49] The same level of theory was used in calculating the electrostatic potentials on the acceptors (see the Supporting Information).

Synthesis and characterization of co-crystals

EDNA was combined with the 15 acceptors in stoichiometric ratios and dissolved in a minimum amount of methanol and kept in vials for slow evaporation in order to obtain co-crystals suitable for single crystal X-ray diffraction (see the Supporting Information for

X-ray experimental details). Once the crystals were obtained they were analyzed using IR spectroscopy and DSC to identify potential co-crystals (see the Supporting Information). From the initial screening with IR and DSC eight out of 15 experiments produced co-crystals. Out of the eight co-crystals obtained, six yielded crystals suitable for single-crystal diffraction: **EDNA:A3**, **EDNA:A4**, **EDNA:A5**, **EDNA:A7**, **EDNA:A8** and **EDNA:A12**. Thermal properties of all eight co-crystals were obtained using DSC data and detonation properties were calculated for the six compounds for which experimental densities were available from crystallographic data. For the co-crystals **EDNA:A3**, **EDNA:A4**, **EDNA:A5** and **EDNA:A8** room temperature unit cells and room temperature densities were determined.

Impact sensitivity

Impact sensitivities of EDNA, **EDNA:A3** and **EDNA:A8** were measured by impact drop testing. The tests were carried out using an apparatus designed to accommodate small amounts of material[50] and was calibrated against tetranitromethane (H_{50} 39(±1) cm). Approximately 0.2 mg of each sample was sealed into aluminum DSC pans. A freefalling 5 lb weight was used to strike the samples from different heights measured in centimeters, which subsequently allowed us to calculate the H_{50}, the height at which the material exhibited a 50% chance of detonation using value using Bruceton analysis.[51] It must be stated that this is a nonstandard testing apparatus and the results obtained are useful for relative comparisons only.

Acknowledgements

This material is based upon work supported by, or in part by, the US Army Research Laboratory and the US Army Research Office under contract/grant number W911NF-13-1-0387.

Keywords: co-crystals · crystal engineering · energetic materials · ethylenedinitramine · hydrogen bonds

[1] a) D. Guo, Q. An, W. A. Goddard, S. V. Zybin, F. Huang, *J. Phys. Chem. C* **2014**, *118*, 30202 – 30208; b) T. Yan, K. Wang, X. Tan, J. Liu, B. Liu, B. Zou, *J. Phys. Chem. C* **2014**, *118*, 22960 – 22967.

[2] a) J. H. Urbelis, J. A. Swift, *Cryst. Growth Des.* **2014**, *14*, 1642 – 1649; b) K. B. Landenberger, A. J. Matzger, *Cryst. Growth Des.* **2010**, *10*, 5341 – 5347.

[3] a) D. I. A. Millar, H. E. Maynard-Casely, D. R. Allan, A. S. Cumming, A. R. Lennie, A. J. Mackay, I. D. H. Oswald, C. C. Tang, C. R. Pulham, *CrystEngComm* **2012**, *14*, 3742 – 3749; b) C. Wei, H. Huang, X. Duan, C. Peia, *Propellants Explos. Pyrotech.* **2011**, *36*, 416 – 423; c) C. Ma, Z. Liu, Q. Yao, *Can. J. Chem.* **2014**, *92*, 803 – 808.

[4] a) C. He, J. Zhang, D. A. Parrish, J. M. Shreeve, *J. Mater. Chem. A* **2013**, *1*, 2863 – 2868; b) C. J. Underwood, C. Wall, A. Provatas, L. Wallace, *New J. Chem.* **2012**, *36*, 2613 – 2617.

[5] a) K. B. Landenberger, A. J. Matzger, *Cryst. Growth Des.* **2012**, *12*, 3603 – 3609; b) G. H. Tao, Y. Guo, Y. H. Joo, B. Twamley, J. M. Shreeve, *J. Mater. Chem.* **2008**, *18*, 5524 – 5530.

[6] G. Chen, W. Shi, M. Xia, W. Lei, F. Wang, X. Gong, *J. Mol. Model.* **2014**, *20*, 2326.

[7] Y. Wang, Z. Yang, H. Li, X. Zhou, Q. Zhang, J. Wang, Y. Liu, *Propellants Explos. Pyrotech.* **2014**, *39*, 590 – 596.

[8] a) M. M. Qasim, B. Moore, L. Taylor, P. Honea, L. Gorb, J. Leszczynski, *Int. J. Mol. Sci.* **2007**, *8*, 1234 – 1264; b) V. K. Balakrishnan, A. Halasz, J. Hawari, *Environ. Sci. Technol.* **2003**, *37*, 1838 – 1843; c) J. Zhang, C. He, D. A. Parrish, J. M. Shreeve, *Chem. Eur. J.* **2013**, *19*, 8929 – 8936.

[9] D. Fischer, T. M. Klapötke, D. G. Piercey, J. Stierstorfer, *Chem. Eur. J.* **2013**, *19*, 4602 – 4613.

[10] a) P. Vishnoi, M. G. Walawalkar, R. Murugavel, *Cryst. Growth Des.* **2014**, *14*, 5668 – 5673; b) Y. Ma, A. Zhang, C. Zhang, D. Jiang, Y. Zhu, C. Zhang, *Cryst. Growth Des.* **2014**, *14*, 4703 – 4713; c) H. Li, Y. Shu, S. Gao, L. Chen, Q. Ma, X. Ju, *J. Mol. Model.* **2013**, *19*, 4909 – 4917.

[11] a) Y. Ma, A. Zhang, X. Xue, D. Jiang, Y. Zhu, C. Zhang, *Cryst. Growth Des.* **2014**, *14*, 6101 – 6114; b) X. Liu, Z. Su, W. Ji, S. Chen, Q. Wei, G. Xie, X. Yang, S. Gao, *J. Phys. Chem. C* **2014**, *118*, 23487 – 23498; c) J. P. Shen, X. H. Duan, Q. P. Luo, Y. Zhou, Q. Bao, Y. J. Ma, C. H. Pei, *Cryst. Growth Des.* **2011**, *11*, 1759 – 1765.

[12] A. P. Agrawal, *Prog. Energy Combust. Sci.* **1998**, *24*, 1 – 30.

[13] T. M. Klapötke, D. G. Piercey, J. Stierstorfer, *Eur. J. Inorg. Chem.* **2013**, 1509 – 1517.

[14] a) O. Bolton, A. J. Matzger, *Angew. Chem. Int. Ed.* **2011**, *50*, 8960 – 8963; *Angew. Chem.* **2011**, *123*, 9122 – 9125; b) Z. Yang, H. Li, H. Huang, X. Zhou, J. Li, F. Nie, *Propellants Explos. Pyrotech.* **2013**, *38*, 495 – 501.

[15] a) S. R. Anderson, D. J. am Ende, J. S. Salan, P. Samuels, *Propellants Explos. Pyrotech.* **2014**, *39*, 637 – 640; b) H. R. Li, Y. J. Shu, C. Song, L. Chen, R. J. Xu, X. H. Ju, *Chin. Chem. Lett.* **2014**, *25*, 783 – 786.

[16] C. Guo, H. Zhang, X. Wang, X. Liu, J. Sun, *J. Mater. Sci.* **2013**, *48*, 1351 – 1357.

[17] K. B. Landenberger, O. Bolton, A. J. Matzger, *Angew. Chem. Int. Ed.* **2013**, *52*, 6468 – 6471; *Angew. Chem.* **2013**, *125*, 6596 – 6599.

[18] C. Zhang, Z. Yang, X. Zhou, C. Zhang, Y. Ma, J. Xu, Q. Zhang, F. Nie, H. Li, *Cryst. Growth Des.* **2014**, *14*, 3923 – 3928.

[19] C. B. Aakeröy, T. K. Wijethunga, J. Benton, J. Desper, *Chem. Commun.* **2015**, *51*, 2425 – 2428.

[20] H. Xue, G. Ye, B. Twamley, J. M. Shreeve, *Chem. Mater.* **2005**, *17*, 191 – 198.

[21] G. C. Hale, US Patent 2.011.578, **1935**, Dover, N.J. .

[22] United States Department of the Army Technical Manual, *Military Explosives*, Department of the Army, **1989**.

[23] B. T. Fedoroff, O. E. Sheffield, *Encyclopedia of Explosives and Related Items, Vol. 6*, Picatinny Arsenal, **1974**.

[24] M. S. Kettner, T. M. Klapötke, T. G. Müller, M. Suc’eska, *Eur. J. Inorg. Chem.* **2014**, 4756 – 4771.

[25] a) H. S. Jadhav, M. B. Talawar, R. Sivabalan, D. D. Dhavale, S. N. Asthana, V. N. Krishnamurthy, *J. Hazard. Mater.* **2007**, *143*, 192 – 197; b) G. Hervé, C. Roussel, H. Graindorge, *Angew. Chem. Int. Ed.* **2010**, *49*, 3177 – 3181; *Angew. Chem.* **2010**, *122*, 3245 – 3249.

[26] J. C. Hinshaw, W. W. Edwards, W. W. George, J. Gilardi, *Heterocycl. Chem.* **1992**, *29*, 1721 – 1724.

[27] L. I. Bagal, M. S. Pevzner, A. N. Frolov, N. I. Sheludyakova, *Khim. Geterotsikl. Soedin.* **1970**, 558 – 562.

[28] R. Meyer, J. Köhler, A. Homburg, *Explosives*, Wiley-VCH, Weinheim, **2008**.

[29] V. P. Ivshin, T. N. Ivshina, L. G. Smirnova, M. G. Ponomareva, *Zh. Org. Khim.* **1984**, *20*, 7 – 13.

[30] M. Robert, J. Pachman, *Primary Explosives*, Springer, Heidelberg, **2013**.

[31] R. W. Millar, Lead-Free Initiator Materials for Small Electro-explosive Devices for Medium Caliber Munitions, QineiQ/FST/CR032702/1.1, **2003**.

[32] A. O. Franz, US 2708623A, **1955**, Olin Mathieson Chemical Corporation, Virginia.

[33] J. W. Turley, *Acta Crystallogr. Sect. B* **1968**, *24*, 942 – 946.

[34] C. B. Aakeröy, S. Panikkattu, B. DeHaven, J. Desper, *CrystEngComm* **2013**, *15*, 463 – 470.

[35] Q. L. Yan, S. Zeman, J. Šelešovský, R. Svoboda, A. Elbeih, *J. Therm. Anal. Calorim.* **2013**, *111*, 1419 – 1430.

[36] a) B. Yan, N. N. Zhao, H. X. Ma, J. R. Song, F. Q. Zhao, R. Z. S. Hu, *S. Afr. J. Chem.* **2013**, *66*, 136 – 139; b) M. J. Kamlet, H. Hurwitz, *J. Chem. Phys.* **1968**, *48*, 3685 – 3692; c) M. J. Kamlet, S. J. Jacobs, *J. Chem. Phys.* **1968**, *48*, 23 – 35.

[37] J. Barton, *Dust Explosion Prevention and Protection*, IChemE, Rugby, **2002**.

[38] P. Patnaik, *A Comprehensive Guide to the Hazardous Properties of Chemical Substances*, Wiley, New York, **2007**.

[39] S. Li, Q. Li, R. Li, R. Liu, K. Yang, B. Liu, B. Zou, *J. Phys. Chem. C* **2014**, *118*, 23443 – 23450.

[40] a) H. Wei, H. Gao, J. M. Shreeve, *Chem. Eur. J.* **2014**, *20*, 16943 – 16952; b) P. F. Pagoria, G. S. Lee, A. R. Mitchell, R. D. Schmidt, *Thermochim. Acta* **2002**, *384*, 187 – 204.

[41] CSD ConQuest 1.17, **2013** Cambridge Crystallographic Data Centre, UK.
[42] D. M. Badgujar, M. B. Talawar, S. N. Asthana, P. P. Mahulikar, *J. Hazard. Mater.* **2008**, *151*, 289–305.
[43] T. K. Highsmith, J. M. Hanks, S. P. Velarde, J. C. Battaro, WO02060881, **2002**, Alliant Techsystems Inc, Virginia.
[44] C. B. Aakeröy, T. K. Wijethunga, J. Desper, *CrystEngComm* **2014**, *16*, 28–31.
[45] N. Iranpoor, H. Firouzabadi, D. Khalili, S. Motevalli, *J. Org. Chem.* **2008**, *73*, 4882–4887.
[46] N. R. Ayyangar, S. N. Naik, K. V. Srinivasan, *Tetrahedron Lett.* **1989**, *30*, 7253–7256.
[47] T. M. Klapötke, B. Krumm, F. X. Steemann, G. Steinhauser, *Safety Sci.* **2010**, *48*, 28–34.
[48] L. W. Kissinger, M. J. Schwartz, *Org. Chem.* **1958**, *23*, 1342–1344.
[49] Spartan′08, Wavefunction, Inc.
[50] O. Bolton, L. R. Simke, P. F. Pagoria, A. J. Matzger, *Cryst. Growth Des.* **2012**, *12*, 4311–4314.
[51] a) K. B. Landenberger, O. Bolton, A. J. Matzger, *J. Am. Chem. Soc.* **2015**, *137*, 5074–5079; b) L. R. Simpson, M. F. Foltz, *LLNL Small-Scale Drop-Hammer Impact Sensitivity Test*, Lawrence Livennore National Laboratory.

Received: May 2, 2015